Effect of Molecular Binding to a Semiconductor on Metal/Molecule/Semiconductor Junction Behavior

ARTICLE *in* THE JOURNAL OF PHYSICAL CHEMISTRY B · JUNE 2005

Impact Factor: 3.3 · DOI: 10.1021/jp0504470 · Source: PubMed

Effect of Molecular Binding to a Semiconductor on Metal/Molecule/Semiconductor Junction Behavior

Hossam Haick,[†] Jamal Ghabboun,[†] Olivia Niitsoo,[†] Hagai Cohen,[‡] David Cahen,*[,†] Ayelet Vilan,[§] Jaehyung Hwang,[||] Alan Wan,[||] Fabrice Amy,[||] and Antoine Kahn*[,||]

Department of Materials and Interfaces and Chemical Support Services, Weizmann Institute of Science, Rehovot 76100, Israel, Ilse Katz Center for Nanotechnology, Ben-Gurion University, Beer-Sheva, 84105, Israel, and Department of Electrical Engineering, Princeton University, Princeton, New Jersey 08544

Received: January 25, 2005; In Final Form: March 5, 2005

Diodes made by (indirectly) evaporating Au on a monolayer of molecules that are adsorbed chemically onto GaAs, via either disulfide or dicarboxylate groups, show roughly linear but opposite dependence of their effective barrier height on the dipole moment of the molecules. We explain this by Au−molecule (electrical) interactions not only with the exposed end groups of the molecule but also with its binding groups. We arrive at this conclusion by characterizing the interface by in situ UPS-XPS, ex situ XPS, TOF-SIMS, and Kelvin probe measurements, by scanning microscopy of the surfaces, and by current−voltage measurements of the devices. While there is a very limited interaction of Au with the dicarboxylic binding groups, there is a much stronger interaction with the disulfide groups. We suggest that these very different interactions lead to different (growth) morphologies of the evaporated gold layer, resulting in opposite effects of the molecular dipole on the junction barrier height.

1. Introduction

The design, preparation, and study of the physical properties of molecular assemblies and organic molecule-based materials that exhibit interesting chemical, physical, or spectroscopic properties is an active area of research.[1] The quest in this area is not only for molecule-based compounds that behave as classical semiconductors but also to produce materials and systems that may exhibit new (combinations of) properties. By judicious choice of the molecular building blocks, one can indeed combine, in the same crystalline framework, two or more properties that are difficult to achieve in a one-phase solid.[2]

The adsorption of tailor-made organic molecules onto solid surfaces and the ability to contact them electrically can lead to hybrid molecular/nonmolecular systems that combine the cooperative (electron transport) properties of these solids and the controllable functional versatility of the molecules.[3] If these materials are used in electrical devices, the nature of the electrical contact to the molecules is found to be crucial for the resulting electronic characteristics.[2,4]

The importance of metal−molecule contacts is also clear from research on organic thin film devices, for example, field effect transistors[5,6] and photovoltaic cells,[7] where an understanding of metal−organic contacts is crucial. Electrical interactions between (inorganic) metals and organics (molecules and polymers) have been studied extensively by in situ ultraviolet photoemission spectroscopy (UPS), X-ray photoelectron spectroscopy (XPS), and Kelvin probe measurements, following the deposition of molecules on metallic substrates and of metal layers on organic thin films.[8−10] These techniques show that molecules interact with the metal in several ways, namely, metal polarization, coupling of electronic states, partial charge exchange (ionic bond formation), or formation of new chemical species,[8−11] affecting the alignment of the energy levels at the interface and as a result the charge transport through it.

Metal contacts to monomolecular films can be expected to show similarities to those made to bulk organic solids, and, indeed, interesting results are being obtained with metal/molecule/substrate systems. Still, few systematic studies have been made, primarily because of the problem in making the metal contacts reproducibly (cf. ref 12). Previously, we have studied contacts by inserting members of a series of molecules whose dipole can be changed systematically, at a metal/semiconductor interface, and probe the resulting electrical characteristics.[13−16] Such molecules generally share the same surface binding group and molecular skeleton, while a variable substituent is situated well away from the binding group.[17] Junctions made with these molecules showed hundreds of millielectronvolt changes in barrier height (or several orders of magnitude in current).[13−16] In addition, we used these series of molecules as a tool to show that the metal deposition mode is crucial for the nature of the molecular effect.

This is so even though the monolayers that they form are far from ideal and likely contain a significant fraction of pinholes.[18,19] The reason is that the electrostatic interactions of the molecular monolayers with the substrate are a relatively long-range effect (on a scale of nanometers). We have shown that if the molecules form even a partial monolayer on a semiconductor, with average dipole orientation perpendicular to the surface, the molecular patches can control the current passing through the junction by means of such electrostatic effects.[18,19] This is because a layer of dipoles affects the interface beyond the lateral dimensions of the molecular domain, that is, into the semiconductor below the adjacent pinhole areas, including regions below the areas located *between* adjacent molecular patches.[18]

Electrical characteristics of a series of dicarboxylic acids on GaAs substrates, contacted by different modes of "ready-made"

[†] Department of Materials and Interfaces, Weizmann Institute of Science.
[‡] Chemical Support Services, Weizmann Institute of Science.
[§] Ben-Gurion University.
[||] Princeton University.

10.1021/jp0504470 CCC: $30.25
Published on Web 04/20/2005

pads, show that the extent to which the molecules' exposed substituents are in proximity to the (top) metallic contact can completely change the electrical characteristics of the resulting devices.[19] This behavior was explained by metal−molecule polarization and partial charge redistribution between the metal and molecules. Additional dipole inversion effects were found to occur between Au and Pd contacts that were *indirectly* evaporated (on a cooled substrate) on the molecules.[20,21] This effect was explained by Au penetration, not only in the intrinsic defects of the monolayer (i.e., the pinholes) but also between closely packed molecules.[20,21] In related work, some inversion of dipole direction upon the adsorption of benzoic acids on a solid substrate (e.g., ITO or Al) was reported.[22] All these effects indicate that the nature of the electrical contact to a molecule, namely, the proximity of the metal to the molecule, and possible metal penetration between molecules, can dominate electron transport measurements, well beyond the effect of contact resistance to molecules, which can also be significant.[23] Here, we report on how the chemical binding group of molecules to a given substrate affects the characteristics of junctions made by vacuum evaporating Au as the contact metal on the molecularly modified semiconductor surface. We use for this two series of systematically varying molecules having different binding groups as our probe. The molecules are adsorbed on GaAs surfaces via carboxylate or disulfide binding groups. To protect the molecules from impinging energetic metal atoms/clusters and, thus, to be able to extract the actual effects that we are interested in, we evaporated Au *indirectly*, on a cooled substrate.

2. Experimental Section

Bare and molecularly modified (100) *n*-GaAs (Si doped, 10^{18} cm^{-3}) surfaces were used. In specific cases, measurements were done also with *p*-GaAs (Zn doped, 10^{18} cm^{-3}). Molecules were synthesized as described elsewhere.[24,25]

2.1. Sample Preparation. GaAs substrates were cleaned by sequential immersion in hot acetone, methanol, and chloroform for 10 min each, followed by ozone oxidation for 10 min (in a UVOCs apparatus). The oxide was removed by a 50 s dip in a NH_4OH/H_2O (1:10 v/v) solution, after which the samples were immersed for 5 s in 18 MΩ deionized water, followed by 5 s immersion in acetonitrile (ACN), and then immediately placed in the adsorption solution.

GaAs surfaces that had been cleaned in this way were modified by overnight adsorption from 2.5 mM solution in ACN with dicarboxylic acids (dC−X)[19,24] or disulfides (dS−X),[25] where X stands for the group opposite the binding group. We will term this group the terminal group, which is, more specifically, the one that determines the free molecule dipole and the one that is directly exposed to the outside, that is, also to the metal that is deposited on the molecules. For both types of molecules, X = OCH_3, H, CN, and CF_3. For dC−X molecules, also X = CH_3 was used. The adsorption or presence of the molecules on the surface was verified by contact angle measurements, ellipsometry, Fourier transform infrared (FTIR) spectroscopy, time-of-flight secondary ion mass spectroscopy (TOF-SIMS), and, for X = CF_3, X-ray photoelectron spectroscopy. In addition, molecular film-induced changes in surface potential were measured as contact potential difference (CPD) by Kelvin probe, as described elsewhere.[13,19,24,25]

Immediately following adsorption, Au was evaporated on the molecularly modified surfaces. For this, the molecularly modified surfaces were introduced into an electron-beam evaporator, *facing away* from the metal source.[18] Evaporation was started after reaching a base vacuum pressure of $(4-6) \times 10^{-7}$ Torr and then refilling the chamber with Ar ($(1.5-1.9) \times 10^{-3}$ Torr) and cooling the sample holder down to 150−200 K. This ensures that only metal atoms and clusters that scattered off Ar atoms or the chamber's walls reach the sample. The effective deposition rates of the Au atoms/clusters on top of the samples were estimated to be 6×10^{-4} to 2×10^{-3} nm/s, respectively. Au film thickness was measured with a quartz crystal monitor. Because of differences in sticking coefficients between the surface of the monitor and that of the sample, the absolute thickness value is a nominal one, but the relative values on one and the same surface are correct. For electrical transport measurements, 30 nm of Au was evaporated. The presence of a cold finger, colder than the sample holder, kept condensation products from accumulating on the sample. This deposition method is called *indirect* evaporation in the remainder of this paper.

2.2. Electrical Characterization. Current−voltage ($I-V$) characteristics were recorded with an HP-4155 semiconductor parameter analyzer between −1 V and +1 V in steps of 10 mV at room temperature. For metal/monolayer/semiconductor structures, the bias was applied between the back Ohmic contact and the Au pad, contacted by a micromanipulator (Karl Suss).

2.3. Scanning Microscopies. Both atomic force microscopy (AFM) and scanning electron microscopy (SEM) were used to look at the morphology of molecularly modified surfaces, onto which we had deposited 0.5, 1, and 2 nm of Au. AFM was done in a semicontact mode, using a Digital Instruments Nanoscope III microscope with standard Si tips (ULTRASHARP, NSC/12/50). SEM was done with a LEO Supra microscope, operated at 2 kV. The differences between the AFM images for samples with 0.5 and 1 nm of deposited Au were too small (or, conversely, the images were too noisy) to allow drawing meaningful conclusions.

2.4. Time-of-Flight Secondary Ion Mass Spectroscopy (TOF-SIMS). TOF-SIMS was used to probe the organic molecules beneath the metal contacts. The experiments were done with a PHI TRIF-II spectrometer. Samples were scanned with a 15 keV Ga^+ beam rastered over a 50×50 μm^2 area to obtain elemental and molecular chemical information on the surface. The signal from Au/monolayer/GaAs structures was referred to that from Au/GaAs ones without molecules.

2.5. Contact Potential Difference (CPD). CPD was measured under ambient (293 K, 40% relative humidity) conditions with a home-built system, based on a Besocke Kelvin probe, to determine the electrical potential of contact-free surfaces relative to that of a (Au) reference,[26] which was taken as 4.9 eV. For molecules on a semiconductor surface, the CPD reflects the work function of the surface, ϕ, that is, the electron affinity, χ, plus the energy difference between the conduction band minimum and the Fermi level (=0.15 eV for the *n*-GaAs used here). The shift in χ, due to a molecular dipole layer, is a function of the molecular dipole moment, μ, and can be expressed as $\Delta\chi = (qN\mu \cos\theta)/\epsilon\epsilon_0$, where q is the electron charge, N is the molecular density, θ is the average tilt of molecules relative to the surface normal, ϵ is the effective dielectric constant of the interfacial layer (i.e., molecular film, surface oxides, etc.), and ϵ_0 is the permittivity of free space.

2.6. Ultraviolet Photoelectron Spectroscopy (UPS) and X-ray Photoelectron Spectroscopy (XPS). UPS and XPS were measured to determine absolute work functions and band bending at the surfaces and interfaces that were studied. The bare and molecularly modified semiconductor samples were mounted on stainless steel or molybdenum plates using silver

paste. Generally, two samples, each with a different molecule adsorbed on it, were mounted side by side on the same plate for direct comparison. These samples were prepared in a N_2-filled glovebox and transferred without ambient exposure to the ultrahigh vacuum system (base pressure of 2×10^{-10} Torr) through a portable N_2-filled vessel. Au was deposited inside the analysis chamber of the photoelectron spectrometer, from a graphite-coated BN crucible. *Indirect* evaporation in an Ar atmosphere (10^{-3} Torr), similar to that described above for normal sample preparation, was used here as well. The samples were cooled to about 263 K during metal deposition, and the deposition rate was 0.02−0.06 nm/min. UPS was performed following every deposition step. Because of potential damage to the molecules by X-rays, in situ XPS was done only after the last metal deposition or on witness samples.

For UPS, we used the He-I (21.22 eV) and He-II (40.8 eV) photon lines from a He-discharge lamp. Photoelectrons were counted with a double-pass cylindrical mirror analyzer. The resolution of the measurement was 150 meV, defined from the Fermi edge measured on a clean polycrystalline Au substrate. XPS was done using the Al Kα (1486.6 eV) line, with a resolution of ∼1.0 eV. The work function of each sample, with and without molecules, was derived from the known position of the Fermi level, measured independently on an Au film, and from the onset of photoemission, which represents the vacuum level of the sample.[27]

Ex situ XPS measurements were carried out with an AXIS-HS Kratos instrument, using a monochromatized Al Kα X-ray source and pass energies ranging from 20 to 80 eV. The resolution was ∼0.5 eV; however, much higher precision could be obtained to determine line shifts, by correlating all the data points of a given set. For the Au 4f core level, shifts down to 10 meV or smaller can be observed in this way. While most measurements were comparative ones between the different samples, the energy scale was calibrated, when needed, using the nonoxidized Ga and As signals from the substrate. Detailed curve fitting was applied using Gaussian−Lorenzian line shapes and Shirley background subtraction.[28] Data were generally taken from fresh, that is, nonirradiated, areas of the sample. Data from repetitive measurements on fixed spots served to determine the relevant time scale of the X-ray beam-induced damage.

3. Results and Discussion

The effect of dicarboxylic (dC−X) acids and disulfides (dS−X) adsorbed on the GaAs side of Au/*n*-GaAs junctions, prepared via *indirect* evaporation of Au, was verified by systematically modifying the functional groups of the molecules. Because of their size and shape (cf. Figure 1), these molecules form incomplete monolayers.[29] Yet, their chemical binding to the substrate ensures that they still have average order, perpendicular to the substrate surface.

Both types of molecules modify the work function of the GaAs by adding an electrostatic potential difference, measured as a change in the CPD, by Kelvin probe. Figure 2 shows that derivatives of dC−X and dS−X monolayers shift the electron affinity, χ, of *n*-GaAs by up to 0.40 and 0.15 eV, respectively. Adding a negative dipole (e.g., with dS−CH_3 and dC−CH_3) decreases χ from that of bare *n*-GaAs, whereas the use of positive molecular dipoles (e.g., with dS−CF_3 and dC−CF_3) increases χ.[30] The effects of both molecule types correlate systematically with the dipole moments of the free molecules. The dipole moments used here were obtained by ab initio calculations, using the B3LYP (DFT) basis sets in Gaussian 98 (cf. ref 31), rather than by the semiempirical (PM3) method used earlier (cf. ref 19).

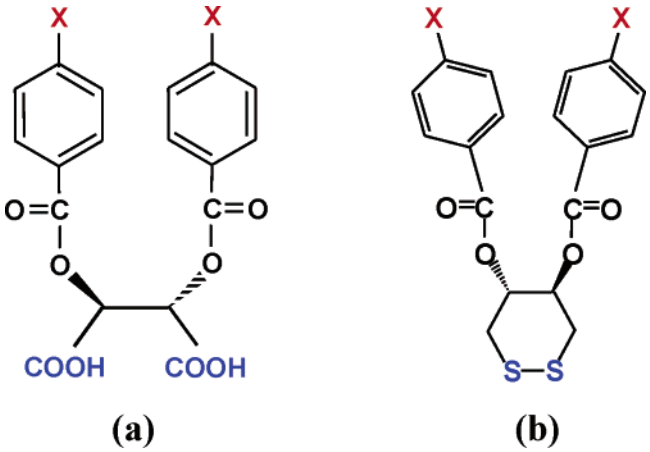

Figure 1. Scheme for the ligands of (a) dicarboxylic acids (dC−X) and (b) disulfides (dS−X) used to modify Au/*n*-GaAs junctions. Changing the ligand substituents ("X" in the scheme) changes the free dipole moment of the molecules. For derivatives of dicarboxylic acid, dC−OCH_3 = −4.3 D, dC−CH_3 = −4.0 D, dC−H = −3.3 D, dC−CN = +3.2 D, and dC−CF_3 = +5.5 D. For derivatives of disulfides, dS−OCH_3 = −6.8 D, dS−H = −4.1 D, dS−CN = +1.1 D, and dS−CF_3 = +4.4 D. The dipole moments were obtained from ab initio quantum chemical calculations, as described in ref 31.

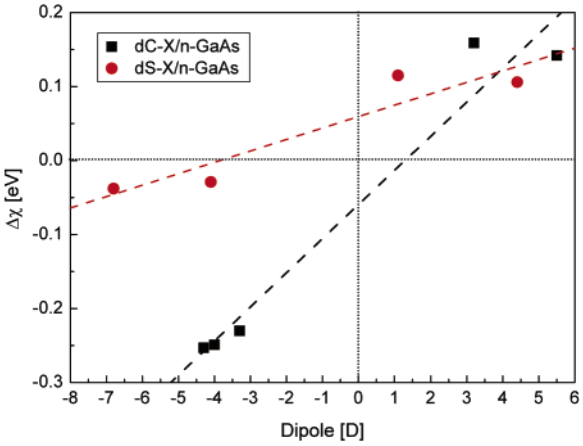

Figure 2. Change in electron affinity of *n*-GaAs, $\Delta\chi$, due to molecule adsorption, as a function of the dipole moment of the substituted ligands of dC−X and dS−X. The dashed lines are best fits to the data. The changes are with reference to bare *n*-GaAs (i.e., $\Delta\chi = \chi_{mol} - \chi_{bare}$). The measured electron affinity of bare samples, χ_{bare}, was ∼4.35 eV. Since each series of junctions, including the bare ones, was pretreated simultaneously, it is likely to ascribe difference between the χ_{bare} values to different oxides on the GaAs surfaces.[30]

TABLE 1: Work Function, ϕ, of GaAs Measured by CPD (the Work Function of the Au Reference Electrode Is Assumed to Be Equal to 4.9 eV) and UPS, Following the Preparation Methods Described in the Experimental Section[a]

	n-GaAs		*p*-GaAs	
	ϕ_{CPD} (eV)	ϕ_{UPS} (eV)	ϕ_{CPD} (eV)	ϕ_{UPS} (eV)
bare	4.2	4.2	4.7	
dC−CH_3	4.0	4.3	4.4	4.5
dC−CF_3	4.4	4.7	4.8	4.9

[a] Differences between absolute values may be due to a larger concentration of surface oxide on the samples measured via Kelvin probe than on the samples, measured by UPS in vacuum. We note the good agreement of the differences in work functions between the DC−CH_3- and DC−CF_3-covered surfaces, obtained from the UPS and Kelvin probe measurements.

Table 1 shows the work function, ϕ, of *n*- and *p*-GaAs measured by CPD and UPS as a function of substituent groups

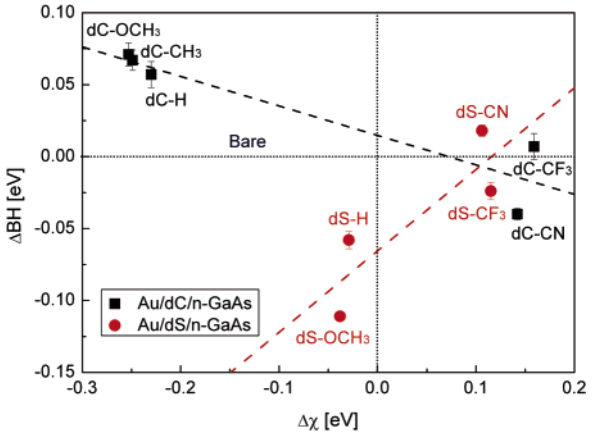

Figure 3. Dependence of the change in the barrier height ($\Delta BH = BH_{mol} - BH_{bare}$) of Au/dC−X/*n*-GaAs and Au/dS−X/*n*-GaAs junctions on the change of the electron affinity ($\Delta\chi = \chi_{mol} - \chi_{bare}$) of the corresponding contact-free molecularly modified surfaces. The dashed lines are best fits to the data. For the bare junctions, BHs of 0.57 and 0.64 eV were found for the experiments reported here for the dC−X and dS−X series, respectively. Differences in electron affinity of the bare surfaces and in the BH of the junctions made with them are due to variations in the oxide on the GaAs surfaces, due to the ambient conditions (~291−295 K and relative humidity of ~20−40%).

of the dC−X molecule. Changes in the work function, $\Delta\phi$, between surfaces modified by dC−X layers with X = CH_3 or CF_3, as measured by the two methods are in good agreement.[32] Differences between the absolute ϕ values measured by UPS and those derived from the CPD data are probably due to the oxide that is present (as confirmed by XPS) on the air-exposed samples used for CPD measurements (cf. UHV-UPS).

As reported earlier, the current−voltage ($I-V$) characteristics of Au/molecule/ semiconductor junctions vary systematically with the molecule substituents. Strikingly, though, while modification with both dC−X and dS−X molecules yields large and systematic effects, these are *opposite* to each other. The variation in $I-V$ characteristics is attributed to a change in the (Schottky) barrier height for charge transfer across it. In the thermionic emission model, the current depends exponentially on this barrier height (BH).[33] In the simple Schottky view, the BH, ϕ_b, of a metal/semiconductor junction is determined by the difference between the free metal work function and the free semiconductor electron affinity, via the Schottky−Mott relation, which for an *n*-type semiconductor is given by[34]

$$\phi_b = \phi_{metal} - \chi_{semiconductor} \quad (1)$$

Equation 1 implies that the effect of the adsorbed molecules on the electron affinity of the bare GaAs (cf. Table 1 and Figure 2) should also appear in the expression of the BH of the molecularly modified junction. We verify this in Figure 3, which shows the change in the effective barrier height ($\Delta BH = BH_{mol} - BH_{bare}$) as a function of $\Delta\chi$ (from Figure 2) for the two types of junctions.[30] The effective BH was calculated from the intercept of the best linear fit to the ln(I)−V plots, calculated from the measured $I-V$ curves (i.e., assuming thermionic emission as the dominant mechanism for current transport across the interface[18]).

As shown in Figure 3, an increasingly positive $\Delta\chi$ gives an increasingly positive BH for junctions modified with dS−X and an increasingly negative BH for junctions modified with dC−X. The magnitude of the molecular effect on the BH is deduced from $|\gamma| = |\Delta BH/\Delta\chi|$, which is 0.2 and 0.55 for dC−X and dS−X molecules, respectively (note that these values are much larger than the index of interface behavior, $\Delta BH/\Delta\phi$, for GaAs (=0.1), extracted from experiments with metals with varying work function, ϕ,[35] emphasizing the critical role of the molecules).[36] The significantly lower $|\gamma|$ value for dC−X molecules, as compared to the dS−X molecules, mainly reflects the smaller $\Delta\chi$ value upon adsorption of dS−X molecules on the free surface electron affinity.

The observation of a systematic substituent-induced effect on the barrier for both types of molecules shows that the Au evaporation does not damage the outer functional groups of the molecule, as damage to the molecule would disturb it.[21] As soon as patches of Au form, one expects the work function measurement to give an arithmetic average, reflecting the presence of areas covered with Au and areas where the molecules are still exposed. Indeed, systematic trends, due to the systematic variation of molecular dipole moment, obtained by varying the X groups, are retained, as seen by CPD measurements for samples with low nominal Au coverage (less than a few nanometers).[37] The trend in $\Delta\chi$, obtained for the free surfaces after molecule adsorption, is preserved with the dC−X molecules, although, as expected, in a reduced way. For the dS−X molecules, an inversion is observed after 1 nm of Au deposition, corresponding to the opposite, but systematic way in which the dC−X and dS−X molecules affect the BH.[37] This indicates that some additional interaction between the Au, the dS−X molecules, and/or the substrate occurs upon junction formation, as will be discussed in detail in the remainder of this paper.

Although the dC−X and dS−X molecules are very similar (see Figure 1), they bind differently to GaAs, that is, the disulfide to As[38] and the carboxylic acid to Ga.[39] TOF-SIMS and XPS results show that GaAs etching with a dilute NH_4OH solution (see the Experimental Section) leads to a 1.5−2-fold higher concentration of Ga and Ga-oxide than of As and As-oxide. Assuming a homogeneous distribution of the As and Ga sites on the surface, this will lead to a less dense coverage of dS−X than of dC−X molecules (75−85%). Indeed, this agrees with the TOF-SIMS results that show concentrations of COO and S on Ga and As, respectively, after molecule adsorption, comparable to those of exposed Ga and As, before molecule adsorption.

Since the molecules are contacted in the same way, that is, by *indirect* evaporation of Au, the difference in the monolayer effect on the BH can be attributed only to different Au interactions with the GaAs surface and to differences in molecule−surface bonds. We will, therefore, argue that if evaporated Au contacts the molecules, it interacts in the same way (if at all) with a given type of outer end group of the two series of molecules but differently with the molecules at the GaAs interface and, as a result, with the GaAs surface itself. This idea is supported by the behavior of evaporated Au, which is known to diffuse easily between molecules.[20,40]

As a first check, we looked by scanning probe (AFM) and electron microscopies at the surfaces of films with 0.5, 1, and 2 nm of Au deposited on dS- and dC-bound monolayers of $-CF_3$ and $-CH_3$ terminated molecules. With both microscopies, differences were observed. SEM at 1.2×10^6 times magnification showed a smaller grain size at 0.5 nm on the dS−X/GaAs monolayers than on the dC−X/GaAs ones. From 1 nm onward, the Au on the dC−X/GaAs monolayers starts to aggregate, while on the dS−X/GaAs monolayers individual grains continue to dominate also at 1 nm. At 2 nm, the Au seems to form a more uniform monolayer on the dS−X/GaAs monolayers than on the dC−X/GaAs ones. The lower resolution AFM images showed

TABLE 2: Relative Concentrations of Different Chemical Residues Found by TOF-SIMS at Au/dC−X/GaAs and Au/dS−X/GaAs Interfaces[a]

interaction[b]	Au/dC−X/GaAs	Au/dS−X/GaAs
Au_xGa_y	1.00 ± 0.07	1.77 ± 0.09
$Au_xGa_yO_z$	1.00 ± 0.04	3.78 ± 0.14
Au_xAs_y	1.00 ± 0.04	5.46 ± 0.16
$Au_xAs_yO_z$	2.60 ± 0.11	1.00 ± 0.08
Au_wS_y	1.00 ± 0.06	2.31 ± 0.13

[a] All results are normalized for the coverage of dC−X and dS−X molecules on the GaAs surfaces.[29] [b] *x*, *y*, *z*, and *w* are integer numbers having the following values: $x = 1-5$, $y = 1-2$, $z = 1-6$, and $w = 1-3$.

a larger roughness at 1 and 2 nm of Au on the dC−X/GaAs monolayers than on the dS−X/GaAs ones.

The results of the TOF-SIMS experiments on dC−CF_3/*n*-GaAs and dS−CF_3/*n*-GaAs surfaces, onto which 0.5−1.0 nm of Au was deposited, provide some relevant information. The relative concentrations of the various chemical groups at these interfaces are summarized in Table 2. Some Au−S interaction is detected for both types of junctions. Those detected in the Au/dC−X/GaAs junction are ascribed to contamination/residues on the GaAs surface due to the wet substrate pretreatment. While such residues may exist also at the dS−X junctions, the ∼2-fold higher Au−S signal suggests that Au interacts with the sulfur of the (di)sulfide binding groups. At the same time, no significant Au−C and Au−CO_y signal is detected for Au/dC−X/GaAs, showing that Au does not interact with the carboxylate binding group of the dC−X molecules. In addition, the results show significantly higher Au−As and Au−Ga_yO_z interaction in junctions with dS−X molecules than in those with the dC−X ones, and higher Au−As_yO_z interaction in junctions with dC−X than in those with dS−X molecules.

How, then, can this picture explain the opposite BH trends shown in Figure 3? The dC−X molecules bind to GaAs by means of interaction between their carboxylate groups and the Ga surface sites,[39] whereas the dS−X molecules bind to the substrate via interaction between the sulfide and As surface sites.[38] Therefore, once the dC−X or dS−X molecules are adsorbed on the GaAs, an excess of As or Ga surface sites remains unoccupied, respectively. Part of these sites may get oxidized and form As_yO_z and Ga_yO_z. The (surface sensitive) As 2p and Ga 2p XPS data on Au (0.5 nm)/dC−CF_3/*n*-GaAs and Au (0.5 nm)/dS−CF_3/*n*-GaAs samples show more As−O for the dC- than for the dS-covered surfaces and more Ga−O for the dS- than for the dC-covered ones.[29] These findings are consistent with sulfide bonding to As and carboxylate bonding to Ga.

In junctions containing dC−X molecules, penetration of the Au toward the substrate leads, therefore, to enhanced interaction with As_yO_z.[41] This is energetically favored over other possible interactions at this interface (cf. Table 3). In junctions containing dS−X molecules, Au can interact in three different ways:

(1) Direct Au−S interaction: The Au−S bonding energy (∼190 kJ/mol)[42] is higher than the As−S one (90−140 kJ/mol);[38,43] that is, Au−S is favored.

(2) Direct Au−As interaction after As−S bond breaking: The bonding energy of Au−As (167 kJ/mol)[41] is higher than that of As−S; that is, Au−As is favored.

(3) Au−Ga and Au−Ga_yO_z interactions, which are thermodynamically stable.[44]

Together, mechanisms 1 and 2 suggest that the Au evaporation disconnects the disulfide groups from the GaAs surface. XPS data from the dS−CF_3-covered samples are consistent with

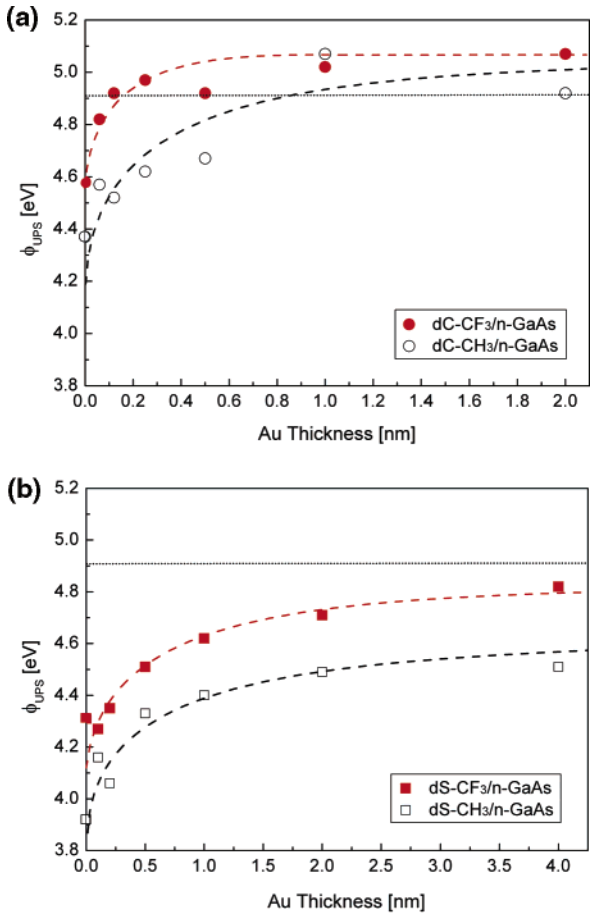

Figure 4. Dependence of the effective work function, derived from the UPS experiments, ϕ_{UPS}, of (a) dC−X/*n*-GaAs and (b) dS−X/*n*-GaAs, on the thickness of the indirectly, in situ evaporated Au film. The Au work function (dotted line) was measured to be 4.9 eV. The dashed lines are best fits to the data.

this interpretation. From the O 1s binding energies, and from the differences in binding energies between Ga 3d and As 3d, oxygen on the surface after Au deposition appears to be more physisorbed, while on the surface without Au it is more oxide-like.[45] Thus, the following picture emerges. Following adsorption of the dS−X molecules, arsenic is bound to S[38] rather than to any oxygen-containing species. Upon Au evaporation, the following process can occur:

$$\text{As}-\text{S}\xrightarrow{\text{Au}}\text{Au}-\ -\text{S} + \text{Au}-\ -\text{As}$$

while, after dC−X adsorption, this will not happen, but rather

$$\text{As}-\text{O}\xrightarrow{\text{Au}}\text{As}-\text{O} + \text{Au}-\ -(\text{As}-\text{O})$$

Upon dS−X adsorption, Ga is oxidized, but in contrast to what is the situation after dC−X adsorption, no strong Ga−O−C bonds are formed. Therefore, after dS−X adsorption,

$$\text{Ga}-\text{O}\xrightarrow{\text{Au}}\text{Au}-\ -\text{Ga} + \text{Au}-\ -(\text{Ga}-\text{O})$$

while, after dC−X adsorption, the strong Ga−O−C link is unaffected by Au evaporation. Ultimately, these processes can lead to a situation where the dS−X molecules become mostly sandwiched between Au electrodes/islands.

To verify these results, the work functions of representative dC−X/ and dS−X/*n*-GaAs surfaces, with X = CH_3 and CF_3, and with metal films of varying thickness on top of them, were

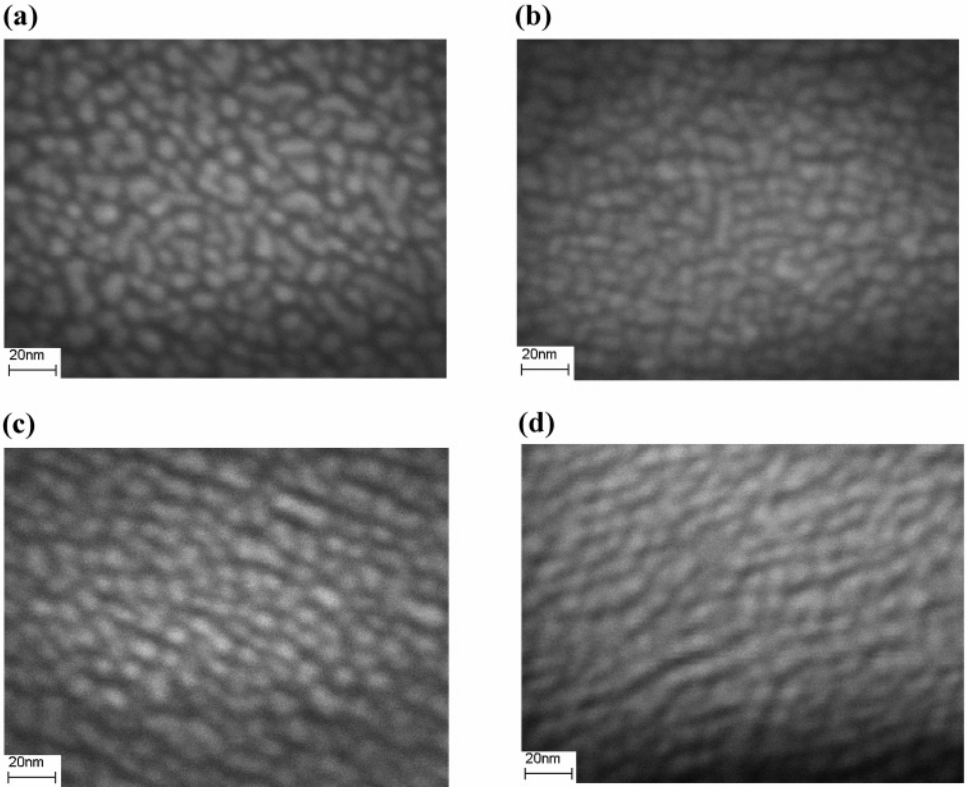

Figure 5. SEM images (at ×1200k magnification) of a Au film with a 0.5 nm nominal thickness, deposited on (a) dC−CF_3/GaAs and (b) dS−CF_3/GaAs surfaces, and of a Au film with a 2 nm nominal thickness, deposited on (c) dC−CF_3/GaAs and (d) dS−CF_3/GaAs surfaces.

probed in situ by UPS. The results show that increasing the Au thickness up to ∼1 nm increases the UPS-measured work function, ϕ_{UPS}, of junctions modified with dC−X (Figure 4a). Evaporation of Au thicker than 1 nm gives ϕ_{UPS} values similar to that measured for a bare, continuous layer of Au (4.9 eV). However, although the ϕ_{UPS} values increase as a function of Au thickness on dS−X molecules, the results are rather different (Figure 4b). Evaporation of ∼1 nm Au layer does not eliminate the molecular effect of the dS−X molecules; that is, the work function of the surface remains directly affected by the terminal group and dipole of the molecule. More than 4 nm of Au is required to start observing the disappearance of the dS−X effect and obtain ϕ_{UPS} of the bare Au.

In parallel, work functions were measured on dC−X/*n*-GaAs and dS−X/*n*-GaAs samples with different nominal Au thicknesses, using a Kelvin probe in ambient.[37] The results up until 1 nm are similar to those obtained with UPS. As the Au becomes thicker, spurious effects enter, possibly due to adsorption from the ambient on the Au.

Considering all these data, we suggest that during evaporation Au diffuses between the molecular chains down to the substrate and produces metal columns or nanoparticles between the molecules. On the basis of reference experiments,[46] these appear to be electrically more conducting than the molecules. In support of this, XPS shows only a very small shift (≤25 meV) between the core level of Au deposited on bare GaAs and Au deposited on dC−X- or dS−X-modified GaAs. This indicates the absence of significant charging of these Au species. Also, while flooding the surface with slow electrons (from the electron flood gun) to induce surface charging, no differential charging between the surface (oxide) and the Au is observed. Given the space between adjacent molecules, ∼0.5 nm, we estimate the dimensions of the Au species to be less than 0.5 nm. Therefore, we can view this as Au intercalated within a monolayer matrix.

TABLE 3: Bond Strengths of Different Chemical Species

interaction	bond strength (kJ/mol)	interaction	bond strength (kJ/mol)
As−Ga[54]	167	Au−O[56]	230
As-oxide[38,55]	318	Au−S[42]	167−197
As−S[38,43]	92−138	C−C[57]	607
Au−As[41]	167	C−S[57]	699
Au−(oxide of) As[44]	653	C−O[58]	105
Au−C[54]	368−377	Ga−O[59]	105−126
Au−Ga[54]	84	Ga−S[42]	59
Au−(oxide of) Ga[44]	1079	Ga-oxide[38]	96

This view fits recent results on well-ordered and dense alkanethiol monolayers, contacted with evaporated Au.[47]

In the dC−X case, Au that diffuses into the monolayer is present primarily as metal atoms and clusters within the layer. Only small amounts of Au are accommodated in the molecular layer, as 1 nm of evaporated Au suffices to conceal the molecular dipole effect on the UPS signal. This explains that the work function rapidly converges toward that of Au (Figure 4a). The buildup of metallic atoms/nanoparticles stops after the dC−X monolayer is saturated with intercalated Au. On the dS−X films, however, diffusion of Au atoms underneath the molecules is significant, because of the above-mentioned chemical reactions with As and S. This depletes the intercalated Au. Therefore, Au that diffuses into the dS−X monolayer is present primarily as As−S−Au and/or As−O−Au compounds, under the dS−X monolayer. This is compatible with the Au XPS data mentioned above. The Au bonding is very mixed, and the various bond strengths of Au with the species present at the interface are not sufficiently different to cause significant core level chemical shifts in our experiment (cf. Table 3). The UPS findings that the dS−X molecular effect on the work function remains detectable even after depositing an amount equivalent to ∼4 nm (Figure 4b) indicates that the monolayer can accommodate a relatively large amount of Au between and

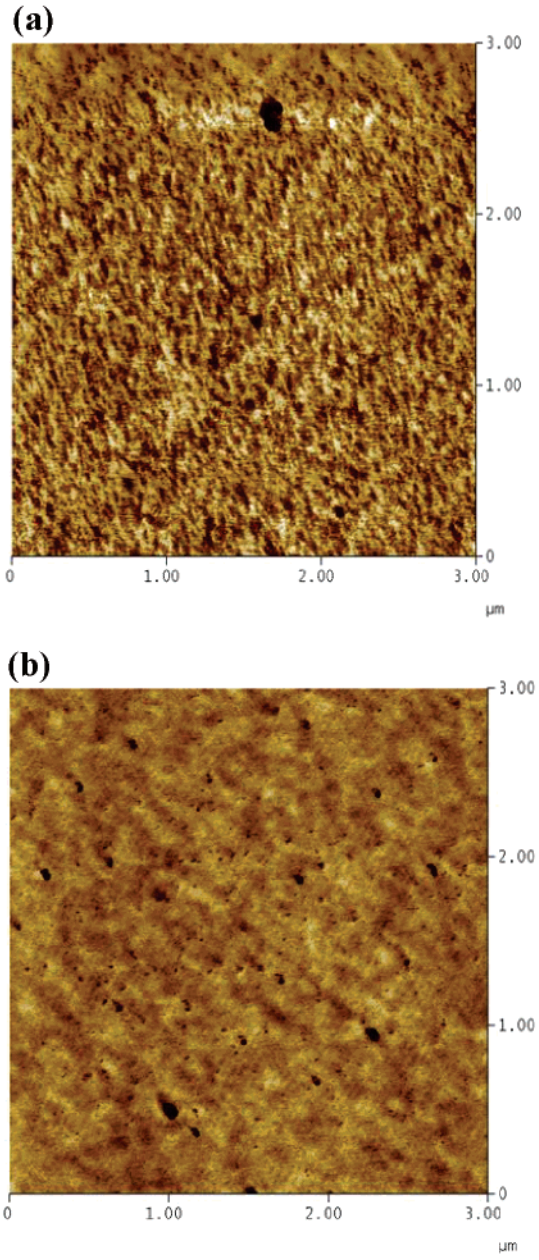

Figure 6. 3 μm × 3 μm AFM scans for Au films of 2 nm nominal thicknesses, deposited on (a) dC−CF_3/GaAs and (b) dS−CF_3/GaAs surfaces. At this nominal thickness, the roughness of Au on dC−X is higher than that on dS−X, with an average cluster height variation of 4.0 and 3.0 nm, respectively.

underneath the molecules, at the interface with GaAs. The formation of a metallic Au layer covering the dS−X molecules is a much slower process than is the case with the dC−X molecules, where already at 1 nm nominal thickness the Au growing out of the pinholes gives the work function of metallic Au.

The AFM and, especially, SEM data are compatible with such a picture. SEM images showed in the case of Au, at 0.5 and 1 nm thickness larger, mostly elongated grains on the dC−X/GaAs surfaces than on the dS−X/GaAs ones (8.0 vs 6.5 nm average length). This is likely due to Au grains aggregating more on dC−X/GaAs than on dS−X/GaAs surfaces (cf. Figure 5a,b for the 0.5 nm Au images). At 2 nm nominal thickness, the dS−X/GaAs surfaces are more completely covered with Au than are the dC ones (cf. Figure 5c,d). Also, the AFM images (Figure 6), which were of significantly better quality for the 2

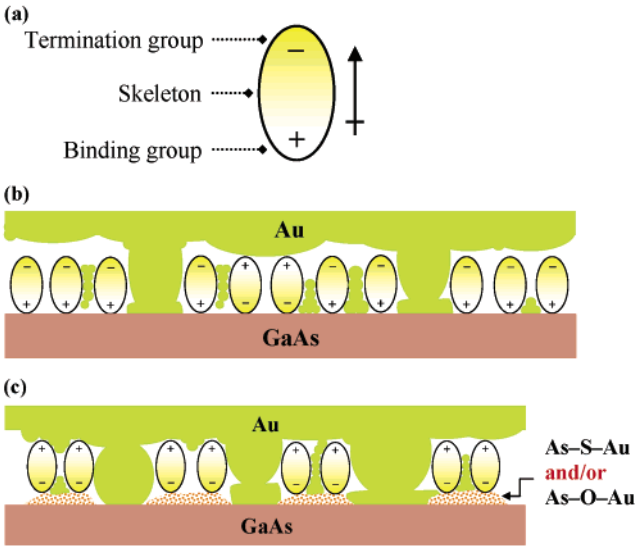

Figure 7. Schematic cross section for (a) the charge distribution of a representative, electron-withdrawing substituent on a *free* dC−X or dS−X molecule (e.g., dC−CF_3 or dS−CF_3) and for the nature of the contact between the metal and (b) dC−X and (c) dS−X molecules on GaAs.

nm Au samples than for the 1 and 0.5 nm ones, show this. Those images also show that the dC−X/GaAs surfaces are rougher than the dS−X/GaAs ones. All these observations are consistent with the above-stated model of stronger Au penetration into the dS−X/GaAs molecular layer than into the dC−X/GaAs one. The reason that Au-covered dS−X/GaAs layers take on the metallic Au work function at higher nominal Au thickness than Au on dC−X/GaAs layers is likely that the more uniform Au film on the dS−X/GaAs surfaces needs to be thicker before showing actual metallic Au behavior, than what is the case on the dC−X/GaAs surface, covered with larger grains.

One possible explanation for such behavior is the following. The growth of Au is typically three-dimensional (3D) because of poor wetting properties. Such growth typically yields larger sized clusters than the two-dimensional (2D) growth of, for example, Pd[48] (indeed, we observe that the deposition of Pd leads to the formation of smoother, films[49,50]). The presence of elongated Au clusters on the dC−CF_3 surfaces, as shown in Figure 5a, supports this point.[51,52] We can then postulate the following: On dC−X monolayers most of the evaporated Au *atoms* and clusters accumulate in the pinholes that are particularly suitable for 3D growth. The Au that lands on the molecules diffuses mainly laterally, toward the pinhole growth centers, in addition to some vertical diffusion into the monolayer.[47] On the basis of the UPS data, the latter process appears to be slow, probably due to the absence of a strong driving force of the type proposed in the case of the dS−X monolayers. The results of Figure 3 can then be explained if most of the layer grows in and on pinholes, overgrowing the space between them. This leads to a rather rough interface with voids between the Au and the molecules (Figure 7b). Under such voids, metal-induced polarization of the end groups is negligible and, therefore, the original direction of charge distribution on the molecule is preserved.

For dS−X layers, the reaction of Au with S and As at the molecule/GaAs interface provides a chemical driving force for Au penetration. This postulate agrees with the UPS data and the SEM images (Figure 5b,d), which, in turn, show the presence of smaller Au clusters (at 0.5 nm) that lead, around 2 nm of Au, to better coverage on the dS−X than on the dC−X layers.[51]

This depletes the exposed surface of the molecules of deposited Au. This process occurs in parallel with pinhole filling, as mentioned above for the dC−X molecular layers. It may even dissolve some of the clusters formed at the surface, making the growth on top of the molecules more 2D-like. The net result is the presence of Au-containing islands below the molecules and of an Au film on top that is in intimate contact with the molecules (Figure 7c), leading to dipole inversion because of the same type of polarization effects that explained the differences between the different types of deposited contacts by lift-off, float-on (LOFO).[19]

Some rationalization for this scenario can be obtained from a closer look at how the metal contact is deposited. In metal evaporation, Au atoms and clusters reach the sample surface with minimal kinetic energies, after scattering several times from the Ar gas atoms and the walls. Because of the low "landing energies" of the metal atoms and clusters, the difference in sticking coefficient between the bare GaAs surface and the molecular film[53] is important and the metal preferentially fills the pinholes (10−20 nm in diameter[18]). The end result is that the Au grows as clusters out of the pinholes, with voids between them, on top of the molecular domains. In this scenario, the deposited Au does not yield an intimate contact with the molecules, resulting in a situation similar to that obtained with "slow" LOFO.[19]

Thus, the main difference between dC−X and dS−X layers is that, with the latter, Au atoms that reach the surface first diffuse through the molecular layer and disconnect the (di)-sulfide from the surface. Au clusters that reach the substrate provide an additional reservoir of Au atoms that continue to diffuse through the layer, while at the same time the pinholes are being filled. This scheme could leave intimately contacted Au also on top of the molecules. However, even if this is not the case, the Au-containing islands underneath the molecular layer, connected to the interdiffused metal, suffice for dipole inversion.

4. Conclusions

It has been previously demonstrated by our group and others that the insertion of a dipole-carrying monolayer into a metal/semiconductor interface (Schottky junction) results in hundreds of millielectronvolt changes in barrier height (or several orders of magnitude in current) and that the metal deposition mode is crucial for preserving the molecular effect. Building on this knowledge, we show in this paper that the chemical binding group of the molecule to a given substrate can also affect the current−voltage characteristics of the junctions. Junctions made by vacuum evaporation of Au on GaAs surfaces modified by a monolayer of dC−X and dS−X molecules are investigated. While we find that the evaporation of Au does not affect the carboxylate binding groups, the same evaporation disconnects the (di)sulfide groups from the GaAs surface. We postulate that these two very different interactions produce non-intimate versus intimate contact between the Au and dicarboxylic acid and disulfide molecules, respectively. This interface structural and morphological difference is then used to explain why the same dipole trend in the dC−X and dS−X molecules results in opposite trends in the junction barrier height.

Acknowledgment. We thank Prof. A. Shanzer and his group (WIS) for the dC−X and dS−X molecules and Prof. G. J. M. Martin for guidance with the ab initio calculations. D.C., J.G., and H.H. thank the Israel Science Foundation, the Gerhard M.J. Schmidt Centre for Supramolecular Chemistry (J.G.), and the Minerva Foundation (Munich) (H.H.) for partial support. A.K. thanks the National Science Foundation (DMR-0408589), the MRSEC program of the National Science Foundation (DMR-0213706), and the New Jersey Center for Organic OptoElectronics for partial support of this work. D.C. thanks Princeton University for support and hospitality during his stays as a Visiting Fellow. A.K. thanks the Weizmann Institute's Materials & Interfaces Department for visiting fellowships. We thank Drs Tao He and Yongdong Jin (Weizmann Institute of Science) for help in AFM measurements.

References and Notes

(1) Alivisatos, A. P.; Barbara, P. F.; Castleman, A. W.; Chang, J.; Dixon, D. A.; Klein, M. L.; McLendon, G. L.; Miller, J. S.; Ratner, M. A.; Rossky, P. J.; Stupp, S. I.; Thompson, M. E. *Adv. Mater.* **1998**, *10* (16), 1297.

(2) Cahen, D.; Hodes, G. *Adv. Mater.* **2002**, *14*, 789.

(3) Adams, D. M.; Brus, L.; Chidsey, C. E. D.; Creager, S.; Creutz, C.; Kagan, C. R.; Kamat, P. V.; Lieberman, M.; Lindsay, S.; Marcus, R. A.; Metzger, R. M.; Michel-Beyerle, M. E.; Miller, J. R.; Newton, M. D.; Rolison, D. R.; Sankey, O.; Schanze, K. S.; Yardley, J.; Zhu, X. *J. Phys. Chem. B* **2003**, *107*, 6668.

(4) Hsu, J. W. P.; Loo, Y. L.; Lang, D. V.; Rogers, J. A. *J. Vac. Sci. Technol., B* **2003**, *21* (4), 1928.

(5) Shen, Y.; Hosseini, A. R.; Wong, M. H.; Malliaras G. G. *ChemPhysChem* **2004**, *5*, 16.

(6) Hirose, Y.; Kahn, A.; Aristov, V.; Soukiassian, P.; Bulovic, V.; Forrest, S. R. *Phys. Rev. B* **1996**, *54*, 13748.

(7) Gal, D.; Sone, E.; Cohen, R.; Hodes, G.; Libman, J.; Shanzer, A.; Schock, H.-W.; Cahen, D. *Proc.−Indian Acad. Sci., Chem. Sci.* **1997**, *109*, 487.

(8) Kahn, A.; Koch, N.; Gao, W. *J. Polym. Sci., Part B: Polym. Phys.* **2003**, *41* (21), 2529.

(9) Shen, C.; Kahn, A.; Schwartz, J. *J. Appl. Phys.* **2001**, *90* (12), 6236.

(10) Ishii, H.; Sugiyama, K.; Ito, E.; Seki, K. *Adv. Mater.* **1999**, *11*, 605.

(11) Gensterblum, G.; Hevesi, K.; Han, B.-Y.; Yu, L.-M.; Pireaux, J.-J.; Thiry, P. A.; Caudano, R.; Lucas, A.-A.; Bernaerts, D.; Amelinckx, S.; Van Tendeloo, G.; Bendele, G.; Buslaps, T.; Johnson, R. L.; Foss, M.; Feidenhans'l, R.; Le Lay, G. *Phys. Rev. B* **1994**, *50* (16), 11981.

(12) de Boer, B.; Frank, M. M.; Chabal, Y. J.; Jiang, W.; Garfunkel, E.; Bao, Z. *Langmuir* **2004**, *20*, 1539.

(13) Vilan, A.; Shanzer, A.; Cahen, D. *Nature* **2000**, *404*, 166.

(14) Wu, D. G.; Ghabboun, J.; Martin, J. M. L.; Cahen, D. *J. Phys. Chem. B* **2001**, *105*, 12011.

(15) Salomon, A.; Berkovich, D.; Cahen, D. *Appl. Phys. Lett.* **2003**, *82* (7), 1051.

(16) Selzer, Y.; Cahen, D. *Adv. Mater.* **2001**, *13* (7), 508.

(17) Ashkenasy, G.; Cahen, D.; Cohen, R.; Shanzer, A.; Vilan, A. *Acc. Chem. Res.* **2002**, *35*, 121.

(18) Haick, H.; Ambrico, M.; Ligonzo, T.; Cahen D. *Adv. Mater.* **2004**, *16*, 2145.

(19) Vilan, A.; Ghabboun, J.; Cahen, D. *J. Phys. Chem. B* **2003**, *107*, 6360.

(20) Haick, H.; Ghabboun, J.; Cahen, D. *Appl. Phys. Lett.* **2005**, *86*, 042113.

(21) Haick, H.; Ambrico, M.; Ghabboun, J.; Ligonzo, T.; Cahen, D. *Phys. Chem. Chem. Phys.* **2004**, *6*, 4538.

(22) Carrara, M.; Nuesch, F.; Zuppiroli, L. *Synth. Met.* **2001**, *121*, 1633.

(23) Rampi, M. A.; Whitesides, G. M. *Chem. Phys.* **2002**, *281*, 373.

(24) Cohen, R.; Kronik, L.; Shanzer, A.; Cahen, D.; Liu, A.; Rosenwaks, Y.; Lorenz, K. K.; Ellis, A. B. *J. Am. Chem. Soc.* **1999**, *121* (45), 10545.

(25) Bruening, M.; Cohen, R.; Guillemoles, J. F.; Moav, T.; Libman, J.; Shanzer, A.; Cahen, D. *J. Am. Chem. Soc.* **1997**, *119*, 5720.

(26) Surplice, N. A.; D'Archy, R. J. *J. Phys. E: Sci. Instrum.* **1970**, *3*, 477.

(27) Cahen, D.; Kahn, A. *Adv. Mater.* **2003**, *15* (4), 271.

(28) Shirley, D. A. *Phys. Rev. B* **1972**, *5*, 4709.

(29) TOF-SIMS measurements show higher surface coverage with dC−X (75−85%) than with dS−X (40−45%) molecules on the *n*-GaAs substrate used here.

(30) The plots do not cross the (0,0) point, something that cannot be explained by the different bond polarities (As−S, Ga−O) of the actual binding groups. It may be due to oxide and/or hydroxide binding (due to exposure to the ambient) to those surface atoms that are not involved in the molecular binding, namely, the Ga and the As ones, respectively. For example, one can argue that the (residual) As−O bond (after dC−X binding to Ga) is less polar than the Ga−O one (after dS−X binding to As).

(31) Gershewitz, O.; Grinstein, M.; Sukenik, C. N.; Regev, K.; Ghabboun, J.; Cahen, D. *J. Phys. Chem. B* **2004**, *108* (2), 664.
(32) $\Delta\phi = \Delta\chi$ if the band bending remains constant.
(33) Rhoderick, E. H.; Williams, R. H. *Metal-semiconductor contacts*; Clarendon Press: Oxford, U.K., 1988.
(34) Sze, S. M. *Physics of Semiconductor Devices*, 2nd ed.; Wiley: New York, 1981.
(35) Tung, R. T. *Mater. Sci. Eng.* **2001**, *R35*, 1.
(36) These values can be compared with those found for Au/dC−X/GaAs junctions, where the Au contacts were prepared by another soft contacting method, lift-off, float-on (LOFO), which gave $\gamma = 0.1$ and $\gamma = 0.55$ for *n*- and *p*-GaAs (cf. ref 19), and for Au/dC−X/*n*-ZnO (LOFO) ones, which gave also $\gamma = 0.55$ (cf. ref 15). In all these cases, $\Delta\chi$, the change in electron affinity upon molecule adsorption, was comparable to that obtained here with the dC−X molecules.
(37) Ghabboun, J. Ph.D. Thesis, Weizmann Institute of Science, 2004.
(38) Lebedev, M. V.; Mayer, T.; Jaegermann, W. *Surf. Sci.* **2003**, *547*, 171.
(39) Bastide, S.; Butruille, R.; Cahen, D.; Dutta, A.; Libman, J.; Shanzer, A.; Sun, L.; Vilan, A. *J. Phys. Chem. B* **1997**, *101*, 2678.
(40) Ohgi, T.; Sheng, H.-Y.; Dong, Z.-C.; Nejoh, H. *Surf. Sci.* **1999**, *442*, 277.
(41) Erkoc, S.; Amirouche, L.; Rouaiguia, L. *Int. J. Mod. Phys. C* **2002**, *13* (6), 759.
(42) Dubois, L. H.; Nuzzo, R. G. *Annu. Rev. Phys. Chem.* **1992**, *43*, 437.
(43) Geib, K. M.; Shin, J.; Wilmsen, C. W. *J. Vac. Sci. Technol., B* **1990**, *8* (4), 838.
(44) Kang, M.-G.; Park, H.-H. *Thin Solid Films* **1999**, *355*−*356*, 435.
(45) Mönch, W. *Semiconductors surfaces and interfaces*, 2nd ed.; Springer: Berlin, 1995; Vol. 26.
(46) In complementary experiments, alkyl (C_{16}) thiol monolayers were adsorbed on Au substrates and contacted by *indirect* evaporation of Au and Pd. The resulting junctions show ∼20% larger number of short-circuits for Au contacts than for Pd ones (cf. ref 20). This is explained by the different mechanism by which Pd grows on the molecules, which will limit metal penetration between the molecular chains. We attribute the higher probability of shorts with Au to the generation of *conductive*, metallic wires between the molecules' chains, in addition to the metals filling the larger pinholes that will be present in such films.
(47) Walker, A.; Tighe, T. B.; Cabarcos, O. M.; Reinard, M. D.; Haynie, B. C.; Uppili, S.; Winograd, N.; Allara, D. L. *J. Am. Chem. Soc.* **2004**, *126*, 3954.
(48) Similar SEM experiments with Pd show no significant differences in terms of the metal film growth on the molecules, between those with dC−X binding groups and those with dS−X ones, a finding that is consistent with the two-dimensional growth of Pd (cf. refs 49 and 50 below).
(49) Li, Y.; DePristo, A. E. *Surf. Sci.* **1996**, *351*, 189.
(50) Schmidt, A. A.; Eggers, H.; Herwig, K.; Anton, R. *Surf. Sci.* **1996**, *349*, 301.
(51) Wang, B.; Xiao, X.; Sheng, P. *J. Vac. Sci. Technol., B* **2000**, *18* (5), 2351.
(52) In the absence of the chemical driving force that stabilizes the deposited Au atoms/clusters on the surface of the molecular film, small *clusters* on top of the monolayer become unstable. As a result, they diffuse, on the monolayer surface, and coalesce into larger, stable clusters, growing in and out of the pinholes. If these are sufficiently close together, these coalesce to form elongated Au islands.
(53) Ulman, A. *An Introduction to Ultra-thin Organic Films*; Academic Press: Boston, MA, 1991.
(54) Barysz, M.; Pyykko, P. *Chem. Phys. Lett.* **1998**, *285*, 398.
(55) Sato, K.; Sakata, M.; Ikoma, H. *Jpn. J. Appl. Phys.* **1993**, *32*, 3354.
(56) Smoes, S.; Manday, F.; Vander Auwera-Manhieu, A.; Drowart, J. *Bull. Soc. Chim. Belg.* **1972**, *81*, 45.
(57) Darwent, B. de B. *Bond Dissociation Energies in Simple Molecules*; NSRDS-NBS 31; National Bureau of Standards: Washington, DC, 1970.
(58) Ranke, W.; Xing, Y. R.; Shen, G. D. *Surf. Sci.* **1982**, *122* (2), 256.
(59) Bock, C. W.; Trachtman, M. *J. Phys. Chem.* **1994**, *98* (1), 95.